Thermophilic versus mesophilic dark fermentation in xylose-fed fluidised bed reactors: biohydrogen production and active microbial community

Paolo Dessì [a,*], *Estefania Porca* [b], *Nicholas R. Waters* [b,c], *Aino-Maija Lakaniemi* [a], *Gavin Collins* [b], *Piet N. L. Lens* [a,d]

[a]*Tampere University of Technology, Faculty of Natural Sciences, P.O. Box 541, FI-33101 Tampere, Finland*

[b]*Microbial Communities Laboratory, School of Natural Sciences, National University of Ireland Galway, University Road, Galway, H91 TK33, Ireland*

[c]*Information and Computational Sciences, The James Hutton Institute, Invergowrie, Dundee, DD2 5DA, Scotland*

[d]*UNESCO-IHE, Institute for Water Education, Westvest 7, 2611AX Delft, The Netherlands*

Manuscript submitted to: *International Journal of Hydrogen Energy*

*Corresponding author: Phone: +358 417239696, e-mail: paolo.dessi@tut.fi, mail: Tampere University of Technology, P.O. Box 541, FI-33101 Tampere, Finland

Abstract

Dark fermentative biohydrogen production in a thermophilic, xylose-fed (50 mM) fluidised bed reactor (FBR) was evaluated in the temperature range 55–70 °C with 5-degree increments and compared with a mesophilic FBR operated constantly at 37 °C. A significantly higher ($p = 0.05$) H_2 yield was obtained in the thermophilic FBR, which stabilised at about 1.2 mol H_2 mol^{-1} xylose (36% of the theoretical maximum) at 55 and 70 °C, and at 0.8 mol H_2 mol^{-1} xylose at 60 and 65 °C, compared to the mesophilic FBR (0.5 mol H_2 mol^{-1} xylose). High-throughput sequencing of the reverse-transcribed 16S rRNA, done for the first time on biohydrogen producing reactors, indicated that *Thermoanaerobacterium* was the prevalent active microorganism in the thermophilic FBR, regardless of the operating temperature. The active microbial community in the mesophilic FBR was mainly composed of *Clostridium* and *Ruminiclostridium* at 37 °C. Thermophilic dark fermentation was shown to be suitable for treatment of high temperature, xylose-containing wastewaters, as it resulted in a higher energy output compared to the mesophilic counterpart.

Keywords: Active community, Biohydrogen, FBR, MiSeq, *Thermoanaerobacterium*, Thermophilic

1. Introduction

H_2 is a carbon free fuel considered as a promising candidate to replace fossil fuels in the near future [1]. Although hydrocarbons are currently the main feedstock for H_2 production, biomass is a renewable and environmentally friendly alternative feedstock [2]. Dark fermentation is the most studied among the biological H_2 production technologies because the variety of usable organic substrates and the high achievable conversion rates may promote the scale-up of the process [3]. However, due to the thermodynamics of the reactions involved, which are more favourable at high temperature and low H_2 partial pressure, operation and optimisation of full-scale dark fermentation is more challenging than traditional anaerobic digestion [4].

Many pathways are possible for dark fermentation, depending on the microbial species, operating parameters, and the substrate used. Glycolysis is the most common route for degradation of hexoses by *Clostridium* [5] and most thermophiles, including *Thermoanaerobacter* [6]. Glucose is oxidized to pyruvate, resulting in the generation of reduced nicotinamide adenine dinucleotide (NADH) and energy in the form of adenosine triphosphate [7]. Pyruvate may be further oxidized to acetylcoenzyme A through reduction of ferredoxin and then to volatile fatty acids (VFAs), or alcohols [7]. Metalloenzymes called hydrogenases use NADH or reduced ferredoxin as electron donor for proton oxidation [8], resulting in the formation of molecular H_2. The oxidation of glucose to H_2 and CO_2 yields 12 mol H_2 mol^{-1} glucose. However, the dehydrogenation of acetate to CO_2 is endergonic, and the spontaneous oxidative process will thus end with acetate production, yielding only 4 mol H_2 mol^{-1} glucose [9]. This thermodynamic limitation is also valid for pentose sugars such as xylose, which will then yield a maximum of 3.33 mol H_2 mol^{-1} xylose.

In practice, the H_2 yield by mixed cultures varies from 14% to 70% of the theoretical limit [10]. For high H_2 partial pressures (> 60 Pa), proton reduction by NADH is not thermodynamically

75 favourable and the reaction switches, e.g. to the butyrate pathway [11], resulting in a lower H_2
76 yield. This can be mitigated by operating dark fermentation in well mixed systems, such as fluidised
77 bed reactors (FBRs), in which the turbulent mixing regime favours the stripping of the produced H_2
78 [12]. Temperature and pH also strongly affect the microbial community and thus, the substrate
79 degradation pathway [13]. Butyrate accumulation can trigger solventogenesis [14], which does not
80 yield H_2. Some microorganisms, including various *Clostridium* sp., are facultative autotrophic and
81 can reduce CO_2 with H_2 forming acetate [10]. Other known H_2-consuming microorganisms include
82 hydrogenotrophic methanogens, propionate producers, and sulphate or nitrate reducing bacteria
83 [15]. Promote the growth of H_2 producers while avoiding the growth of H_2 consuming
84 microorganisms in dark fermentative bioreactors is still an open challenge [16].
85
86 H_2 production at high temperatures can be advantageous in terms of H_2 yield and production rates
87 [17,18]. High temperature positively affects the kinetics of the oxidative reactions and the growth of
88 microorganisms [19]. Furthermore, the direct conversion of sugars to acetate becomes
89 thermodynamically more favourable as the temperature increases, thus resulting in a high H_2 yield
90 [20]. Thermophilic anaerobic microorganisms such as *Thermotoga* and *Thermoanaerobacter* are
91 excellent H_2 producers, as they use most of the reductants produced during glycolysis to form H_2,
92 allowing yields between 3 and 4 mol H_2 mol^{-1} hexose [20]. Although H_2 yields from pure cultures
93 are typically higher [5], mixed cultures are preferable for industrial application, as they offer more
94 stability and versatility, and sterilisation is not required [13]. Most studies on H_2 production at high
95 temperature by mixed cultures have been conducted at 55, 60, or 70 °C, generally obtaining higher
96 H_2 yields than mesophilic trials with a similar inoculum and substrate [18,21,22]. Sources of
97 inoculum used for thermophilic dark fermentation include e.g. sewage sludge [18,23], anaerobic
98 sludge or digestates [21,24–28], animal dung or slurry [29,30], hot spring sediment [31,32], and
99 biomass from previous laboratory-scale H_2 production experiments [33–39].

100 Handling and processing of organic substrates and the low H_2 yield are two of the main deterrents
101 for the establishment of dark fermentation at commercial scale [40]. Despite the higher H_2 yield
102 obtained at high temperatures, the net energy gain (the difference between the energy input needed
103 to heat the reactor and output) seems to be indirectly proportional to the operation temperature [41].
104 However, some industrial wastewaters, such as thermomechanical pulping wastewaters, are
105 produced at high (50–70 °C) temperatures [42] and could be treated in situ avoiding cooling and
106 minimising energy loss. Such wastewaters contain readily fermentable sugars, both hexoses (e.g.
107 glucose) and pentoses (e.g. xylose), suitable for H_2 production by dark fermentation. Continuous
108 dark fermentation of glucose has been widely studied at various temperatures [35,37,39,43,44]
109 while much less attention was given to dark fermentation of xylose, especially at high temperature.
110 In a previous study, H_2 production from xylose was compared in batch cultures at 37, 55 and 70 °C
111 using heat treated (90 °C, 15 min) activated sludge from a wastewater treatment plant as the
112 inoculum [18]. That study showed effective H_2 production at 55 °C, but not at 70 °C. However, the
113 effect of temperature in the 55–70 °C temperature range is worth investigating, as a difference of a
114 few degrees can affect the microbial community inside the reactor and thus, the H_2 production
115 efficiency [44].
116
117 Recently, the establishment of next-generation sequencing techniques has improved the knowledge
118 on H_2-producing microbial communities. Etchebehere et al. [45] performed 454 pyrosequencing on
119 microbiological samples from 20 H_2 producing lab-scale bioreactors operated within a temperature
120 range of 25–37 °C. Although the microbial communities were diverse due to the different operating
121 conditions of the bioreactors, the authors observed a predominance of *Firmicutes* and distinguished
122 high-yield H_2 producers (*Clostridium*, *Kosmotoga*, and *Enterobacter*), low-yield H_2 producers
123 (*Veillonellaceae*) and competitors (*Lactobacillus*). Nitipan et al. [46] reported
124 *Thermoanaerobacterium* as the dominant genus in a thermophilic (60 °C) sequencing batch reactor

producing H_2 from palm oil mill effluent. Zhang et al. [47] showed that *Firmicutes* such as *Caldanaerobius*, *Caldicellulosiruptor* and *Thermoanaerobacter* became dominant in a hyperthermophilic (70 °C) H_2 producing, glucose-fed chemostat. To date, analysis of dark fermentative microbial communities by next-generation sequencing has been mainly based on the presence of 16S rRNA genes, which provides information on the structure of the microbial community. However, an analysis based on the expression of 16S rRNA genes describes more accurately the composition of the microbial community actively involved in dark fermentation [48].

This study aims to evaluate, for the first time, how dark fermentative H_2 production and the composition of the active microbial community are affected by a stepwise (5 °C) temperature increase in the 55–70 °C temperature range in a xylose-fed FBR inoculated with heat treated activated sludge. A second FBR was operated in parallel with the same inoculum, but at a lower temperature (37 °C) in order to compare its performance to the thermophilic counterpart, prior to increasing the temperature to 55 °C to observe the response of this mesophilic microbial community to the temperature shift.

2. Materials and methods

2.1 Source of biomass

Activated sludge was collected from the recirculation line between the aeration tank and the secondary settler in the Viinikanlahti municipal wastewater treatment plant (Tampere, Finland). It was settled, and, after removing the supernatant, heat-treated at 90 °C for 15 minutes as described by Dessì et al. [18] before being used as inoculum for the FBRs.

2.2 Composition of synthetic wastewater

149 Both FBRs were fed with a synthetic wastewater based on the DSMZ 144 medium with xylose (50
150 mM) as electron donor instead of glucose. However, tryptone, resazurin and Na_2S were omitted and
151 the concentration of KH_2PO_4, K_2HPO_4, and yeast extract was reduced 10 times (to 0.55 mM, 0.86
152 mM, and 0.3 g L^{-1}, respectively).
153
154 *2.3 FBR configuration*
155 Two FBRs (Figure 1), 1 L volume each, were operated with 300 mL activated carbon as carrier
156 material for biomass adhesion. A recirculation flow rate of about 1900 mL min^{-1} was applied by
157 using a peristaltic pump (Masterflex, USA) to expand the activated carbon bed by 30% (the flow
158 rate of minimum fluidization was 1400 mL min^{-1}). To maintain a constant expansion, the
159 recirculation flow was increased up to a maximum of 20% due to the adhesion of the biomass,
160 which made the bed heavier. To achieve a stable temperature, the FBRs were operated inside
161 incubators (Labilo, Finland). A water jacket (Julabo, Germany) was also installed, as the heat
162 provided by the incubator was not enough to reach 70 °C inside the FBR.
163
164 To avoid microbial growth, the xylose solution was prepared in a different tank than the medium
165 containing the nutrients and trace elements. Both solutions were flushed with N_2 into the feeding
166 tanks, and their pH was adjusted to 5.0–5.5 with HCl prior to being fed to the FBRs through
167 peristaltic pumps (Masterflex, USA). To minimise the growth of methanogenic archaea [49], the pH
168 inside the reactor was kept at 5 (± 0.1) by automatic titration (Metrohm, Switzerland). The FBRs
169 were sealed on the top, and both liquid and gas were directed to a gas-liquid separator. The liquid
170 was directed to an effluent tank, while the gas was directed to a gas meter (Ritter, Germany) before
171 being released into a fume hood (Figure 1).
172

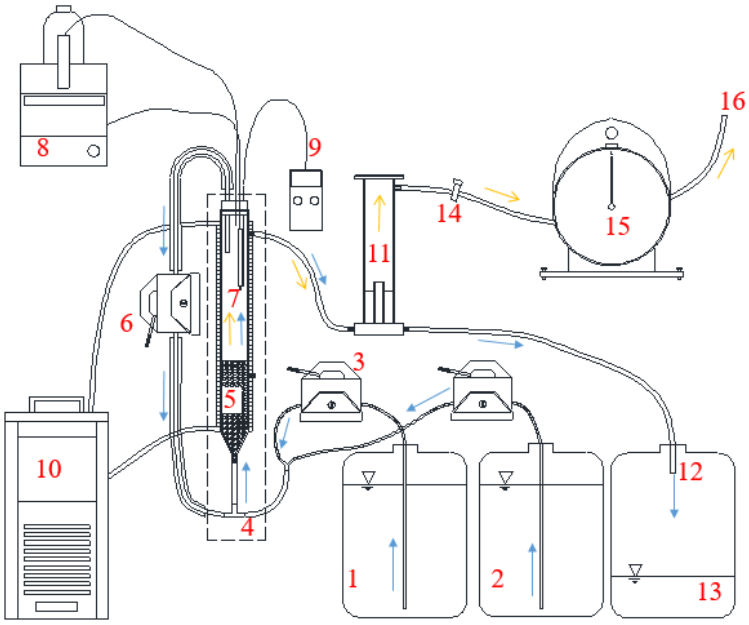

Figure 1. Overview of the experimental set-up used in this study. Medium influent tank (1), xylose influent tank (2), peristaltic pumps for influent feeding (3), influent sampling point (4), activated carbon bed with the active biomass (5), peristaltic pump for recirculation (6), pH probe (7), automatic titrator (8), temperature control (9), water bath (10), gas-liquid separator (11), effluent sampling point (12), effluent tank (13), gas sampling point (14), gas meter (15) and gas outlet (16). Liquid path (↗), gas path (↗). The dashed rectangle represents the part of the set-up located inside the incubator.

2.4 FBR operation and sampling

Both FBRs were inoculated by 50 mL of heat-treated activated sludge (8.8 g VS L^{-1}). After two days of start-up in batch mode, the FBRs were switched to continuous mode (day 0) and operated for 7 days at a hydraulic retention time (HRT) of 12 hours. On day 7, the HRT was decreased to 6 hours. The thermophilic FBR was operated in continuous mode for a total of 185 days. It was initially operated at 55 (± 1) °C. Temperature was then increased to 60 (± 1) °C on day 77, to 65 (± 1) °C on day 119, and to 70 (± 1) °C on day 158 until day 185. The mesophilic FBR was operated at 37 (± 1) °C for 185 days, and then at 55 (± 1) °C until day 228.

Influent and effluent samples and gas samples, were collected from the sampling points specified in Figure 1. Biofilm-containing activated carbon was collected from the thermophilic FBR before every change in operating conditions (plus a mid-term sample collected on day 53), and stored at -20 °C for DNA analysis. Samples from the mesophilic FBR were also collected on the same days. An additional sample of carrier material was collected from the thermophilic FBR on day 119 (60 °C), 158 (65 °C) and 185 (70 °C) and, from the mesophilic reactor on day 185 (37 °C) and 228 (55 °C), and stored at -80 °C for RNA-level analysis. The collection system consisted of a syringe connected to a tube, which was used to suck 4–6 mL of biomass out of the FBR bed. While collecting the biomass samples, the FBRs were open from the top but flushed with N_2 to avoid exposure to air.

2.5 Chemical analysis

Influent and effluent composition was determined either with GC-FID according to Kinnunen et al. [50], or with HPLC as reported by Dessì et al. [18]. Gas samples were analysed for H_2, CH_4, and CO_2 with a Shimadzu gas chromatograph GC-2014 equipped with a Porapak N column (80/100 mesh) and a thermal conductivity detector. Oven, injector and detector temperatures were at 80, 110 and 110 °C, respectively.

2.6 Microbiological analysis

DNA extraction and polymerase chain reaction-denaturing gradient gel electrophoresis (PCR-DGGE) of the partial 16S rRNA gene were performed according to Mäkinen et al. [32]. The forward and reverse primers for PCR were GC-BacV3f and 907r, respectively. The visible bands in the polyacrylamide gel were cut by using a surgical blade, eluted in sterile water and re-amplified by PCR (primers BacV3f and 907r) before sending them to Macrogen (South Korea) for sequencing

215 as described by Koskinen et al. [51]. The nucleotide sequences obtained were analysed using Bio-
216 Edit [52] software version 7.2.5 and compared with the sequences in the GenBank nucleotide
217 collection database using the BLAST software [53].
218
219 Nucleic acids for MiSeq analysis were co-extracted from the biofilm-containing activated carbon
220 samples according to Griffiths et al. [54], but 3M sodium acetate (1/10 of sample volume) and cold
221 (-20 °C) 100% isopropanol (1 sample volume) were added for precipitation instead of polyethelene
222 glycol. Furthermore, nucleic acids were re-suspended in sterile water instead of tris-EDTA buffer.
223 DNA and RNA were quantified by a Nanodrop spectrophotometer (NanoDrop Technologies, USA).
224 Their quality was assessed by measuring the absorbance ratio at 260/280 nm and 260/230 nm
225 wavelength. Nucleic acid samples were diluted to a final concentration of 25 ng mL^{-1}. DNA was
226 removed by adding 1 µL turbo DNase and 2.5 µL turbo DNase buffer (Invitrogen, Thermo Fisher,
227 USA), followed by incubation at 37 °C for 30 minutes. DNase was then inactivated by addition of
228 2.5 µL DNase inactivator (Invitrogen). After centrifugation (10000xg, 1.5 minutes), the RNA-
229 containing supernatant was transferred to a fresh RNase free tube. The absence of DNA was
230 confirmed by 16S rRNA gene PCR (primers 338f and 805r) followed by electrophoresis in 1%
231 agarose gel (no bands obtained).
232
233 Complementary DNA (cDNA) was obtained from RNA using M-MuLV Reverse Transcriptase
234 (New England, BioLabs, USA), following the instructions provided by the supplier. The success of
235 the reverse transcription was confirmed by 16S rRNA gene PCR (primers 338f and 805r) and
236 electrophoresis in 1% agarose gels (bands appeared). Samples of cDNA were sent to FISABIO
237 (Valencia, Spain) for high-throughput sequencing of partial 16S rRNA genes on an Illumina MiSeq
238 platform. Forward and reverse primers for PCR were 515f and 806r, respectively [55]. A total of
239 427,163 raw sequences was obtained from 5 samples. Sequence screening, alignment to Silva

240 (v123) database, clustering, chimeras removal and taxonomic classification (cut-off = 97%) were
241 performed using Mothur v1.39.3 [56], following the procedure described by Kozich et al. [57].
242
243 *2.7 Net energy gain calculation*
244 The net energy gain NE_G (kJ L^{-1}) (Equation 2) was estimated by the difference between the energy
245 E_G recovered by combustion of the H_2 produced per L of wastewater treated (Equation 3) and the
246 energy E_L required to heat the FBR to the desired temperature (Equation 4) [41]:
247
248 Net energy gain: $NE_G = E_G - E_L$ (2)
249 Energy gain: $E_G = Y_H \cdot MV_H \cdot C_X \cdot \rho_H \cdot LHV_H$ (3)
250 Energy loss: $E_L = C_W \cdot (T_F - T_I) \cdot \rho_W$ (4)
251
252 where Y_H is the H_2 yield (mol H_2 mol^{-1} xylose), MV_H is the molar volume of H_2 (22.414 L mol^{-1}),
253 C_X is the influent xylose concentration (50 mol L^{-1}), ρ_H is the density of gaseous H_2 (8.9×10^{-5} kg
254 L^{-1}), LHV_H is the lower heating value of H_2 (120×10^3 kJ kg^{-1}), C_W is the specific heat of water (4.2
255 kJ kg^{-1} K^{-1}), T_F and T_I (K) is the temperature of the wastewater after and before heating,
256 respectively, and ρ_W is the density of water (1 kg L^{-1}).
257
258 *2.8 Statistical analysis*
259 To assess significant differences in H_2 yield at the various temperatures investigated, analysis of
260 variance (ANOVA) and the Tukey test [58] at $p = 0.05$ were conducted using the IBM SPSS
261 Statistics package. The statistical analysis was conducted on the last 4 sampling points collected at
262 the various temperatures investigated in both the mesophilic and thermophilic FBR (8-10 operation
263 days), which were considered a subsample representative of the FBR performance at each
264 temperature. The output of the statistical analysis is provided in the supporting material (File S1).

265

266 **3. Results**

267 *3.1 H_2 production in the thermophilic FBR*

268 For all the temperatures investigated, the thermophilic FBR yielded more H_2 than the mesophilic
269 FBR (Figure 2a versus 2b). At 55 °C (days 1-77), the H_2 yield increased steadily in the first days of
270 operation, reaching 1.2 mol H_2 mol^{-1} xylose on day 18, and remaining relatively stable on days 18–
271 25 (Figure 2a). In the following days, due to a problem with the liquid-gas separator (foam
272 produced by the FBR partially clogged the gas line and part of the gas was likely lost with the
273 effluent), the H_2 yield decreased to a minimum of 0.7 mol H_2 mol^{-1} xylose on day 35. On day 52,
274 after solving the issue by washing the liquid-gas separator, the H_2 yield increased sharply reaching a
275 maximum of about 1.3 mol H_2 mol^{-1} xylose on day 56 and then stabilising to 1.2 mol H_2 mol^{-1}
276 xylose on days 65–77 (Figure 2a). On days 7–77, xylose was detected in the effluent at a
277 concentration < 2.5 mM (> 95% removal). Acetate and butyrate were the main metabolites
278 produced. Their concentration in the effluent increased on days 1–21, reaching a concentration of
279 about 30 and 35 mM for acetate and butyrate, respectively (Figure 2c). Ethanol was produced
280 during the first days of operation, reaching a maximum concentration of about 10 mM on day 7
281 before decreasing to < 2 mM on day 27. On days 65–77, the acetate concentration ranged between
282 20 and 24 mM, while the butyrate concentration ranged between 19 and 25 mM (Figure 2c).

283

284 After increasing the temperature to 60 °C on day 77, the H_2 yield remained stable at 1.2 mol H_2
285 mol^{-1} xylose for one day and then decreased to a minimum of 0.6 mol H_2 mol^{-1} xylose on day 81
286 (Figure 2a). H_2 remained low on days 81–91 and started to increase again, reaching a maximum of
287 about 1.0 mol H_2 mol^{-1} xylose on day 95. From day 98, the H_2 yield slightly decreased again and
288 stabilised to 0.8 mol H_2 mol^{-1} xylose on days 112-119 (Figure 2a). The increase in temperature
289 caused an increase in the VFAs concentration in the effluent (Figure 2c). The acetate concentration

290 almost doubled, ranging between 29 and 42 mM on days 88–119. The butyrate concentration
291 increased as well, ranging between 25 and 35 mM on days 88–119 (Figure 2c).
292
293 At 65 °C (days 120–158), the average H_2 yield was comparable to the yield obtained at 60 °C, but
294 the production was more unstable compared to both 55 °C and 60 °C, ranging between 0.7 and 1.3
295 mol H_2 mol^{-1} xylose (Figure 2a). Increasing the temperature to 65 °C had minimal impact on the
296 VFA concentration when compared to the 60 °C condition (Figure 2c).
297
298 After increasing the temperature further to 70 °C, H_2 production ceased on day 161, but increased
299 again from day 163, stabilising to values comparable to those obtained at 55 °C (1.2 mol H_2 mol^{-1}
300 xylose) on days 172–185 (Figure 2a). A high concentration of xylose was detected in the effluent on
301 days 163–174, with a peak of about 50 mM (0% removal) on day 163. On days 163–174, the
302 acetate and butyrate concentration decreased and slowly increased again, reaching values
303 comparable to the ones obtained at 60 and 65 °C (21–32 mM acetate and 22–32 mM butyrate) on
304 days 175–185 (Figure 2c).
305
306 *3.2 H_2 production in the mesophilic FBR*
307 The mesophilic FBR had a fluctuating H_2 production, especially during days 1–90 (Figure 2b). The
308 H_2 yield was above 1.0 mol H_2 mol^{-1} xylose only on days 53–65. On day 7, 74 and 81, the H_2 yield
309 ceased and increased again within 1–3 days. On days 90–185, the H_2 production fluctuated between
310 0.3 and 1.0 mol H_2 mol^{-1} xylose. Between days 0–185, the xylose concentration in the effluent was
311 < 5 mM (> 90% removal).
312
313 Similar to the H_2 yield, acetate and butyrate production was unstable during days 1–90 (Figure 2d).
314 The acetate concentration was often close to 40 mM and was even higher on day 18 and 76.

315 Interestingly, the peaks of acetate (Figure 2d) seem to mirror the drops in H_2 yield (Figure 2b). On
316 days 90–185, the butyrate concentration ranged between 10 and 19 mM, while the acetate
317 concentration was more unstable, ranging between 20 and 36 mM (Figure 2d).
318
319 After increasing the temperature to 55 °C (day 186), H_2 production ceased on day 206 (Figure 2b),
320 and then increased sharply to values comparable to those obtained in the thermophilic FBR at 55 °C
321 on days 219-228 (1.0 mol H_2 mol^{-1} xylose). After raising the temperature from 37 to 55 °C, xylose
322 was still consumed (> 97%). Ethanol was detected in the effluent on days 195–213, with a
323 maximum of 15 mM on day 208 (Figure 2d). However, the liquid phase composition was similar to
324 the one obtained in the thermophilic FBR at 55 °C on days 217–228 (about 18 and 22 mM acetate
325 and butyrate, respectively).
326
327
328

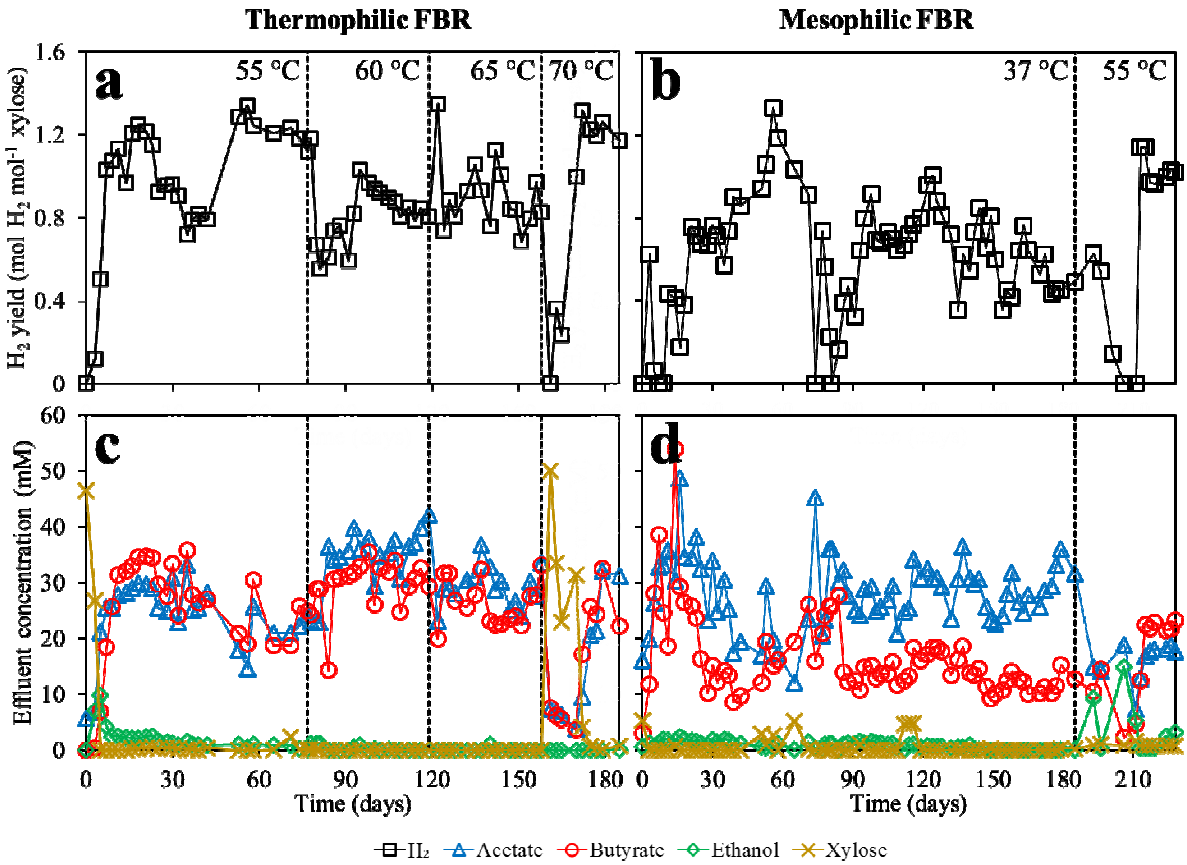

Figure 2. H_2 yield (mol H_2 mol^{-1} xylose added) (a, b) and acetate, butyrate, ethanol and xylose concentration (mM) in the effluent (c, d) of the thermophilic (a, c) and mesophilic (b, d) FBR. The vertical dotted lines indicate a change of temperature.

3.3 Microbial community analysis

Different eubacterial community profiles from the thermophilic and mesophilic FBR were obtained by PCR-DGGE analysis from the biofilm-containing activated carbon (Figure 3; Table 1). In the thermophilic FBR, *Clostridium acetobutylicum* (100% similarity) was found at 55 °C on day 0 (after two days of start-up in batch mode), but was not detected in the subsequent samples (Figure 3). On days 7–185, regardless the temperature, *Thermoanaerobacter thermosaccharolitycum* (98–99% similarity) was the dominant microorganism in the thermophilic FBR (Figure 3). *Alicyclobacillus* sp. (96–97% similarity) was found on day 7, after which its concentration was

342 below detection limit at 55 °C on day 77 and at 60 °C on day 119, but it was detected again when
343 temperature was further increased to 65 and 70 °C (Figure 3).
344
345 A wider eubacterial community was found in the mesophilic FBR compared to the thermophilic
346 FBR. On day 0 and day 7, nucleotide sequences with 99–100% similarity to *Clostridium*
347 *pasteurianum* were detected. Species with 99–100% similarity to *Clostridium acetobutylicum* were
348 detected on all sampling days (days 7–185). On day 77, nucleotide sequences close to
349 *Pseudomonas* and *Delftia* sp. were also found. On days 119, 158, and 185, the DGGE profiles of
350 the mesophilic community were similar to each other and dominated by *Clostridium* sp. (Figure 3).
351
352
353
354

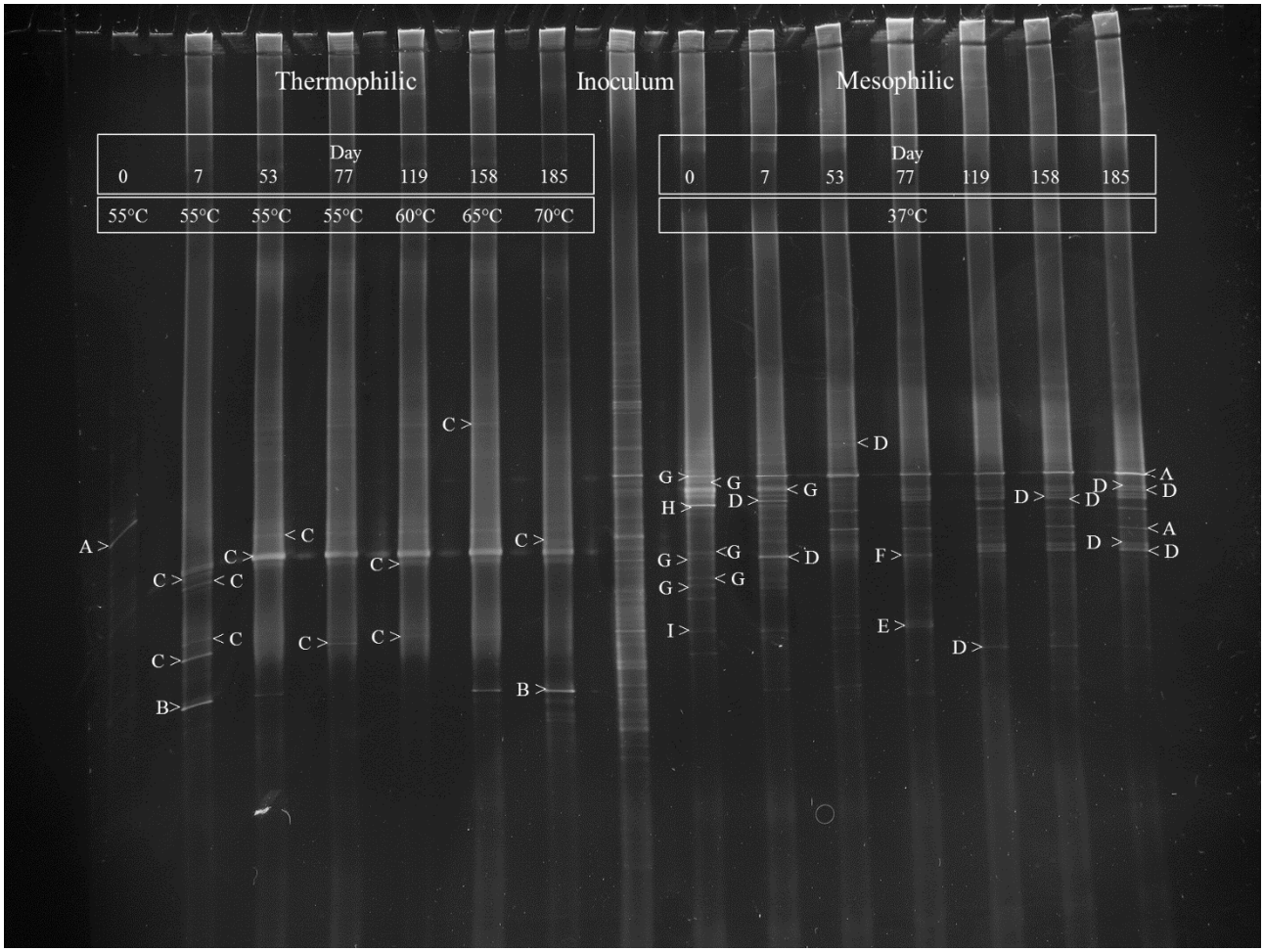

Figure 3. Microbial community profiles obtained by PCR–DGGE from biofilm-containing activated carbon samples collected from the thermophilic and the mesophilic H_2 producing FBR. The band labels refer to Table 1.

368 **Table 1.** Association of 16S rRNA gene sequences of DGGE bands to those collected in the GenBank.

BL[a]	Affiliation[b]	Accession number	Matching sequence lenght[c]	Similarity (%)[d]
A	*Clostridium acetobutylicum*	KP410577 KP410579	446–472	99–100
B	*Alicyclobacillus* sp.	JX505129	485–524	96–97
C	*Thermoanaerobacter thermosaccharolyticum*	JX984968 KJ831072 AF247003	405–499	98–99
D	*Clostridium* sp.	EU887966 EU887970 KU886097 LC020495	367–491	94–99
E	*Pseudomonas* sp.	GQ903481	442	97
F	*Delftia* sp.	KT865666	465	99
G	*Clostridium pasteurianum*	KX378861	440–506	99–100
H	*Ralstonia* sp.	KT183537	496	99
I	*Lysobacter* sp.	JQ791571	429	93

369 [a] Band label in Figure 3a

370 [b] Closest cultured species in GenBank

371 [c] Number of nucleotide pairs used in the sequence comparison

372 [d] Percentage of identical nucleotide pairs between the 16S rRNA gene sequence and the closest species in GenBank

373

374 Based on the high-throughput sequencing of the reverse-transcribed 16S rRNA (Figure 4), species
375 belonging to the *Thermoanaerobacterium* genus dominated the active microbial community (> 99%
376 of the relative abundance) of the thermophilic FBR at both 60 and 70 °C (days 119 and 185). At 65
377 °C (day 158), about 22% of the relative abundance matched the genus *Clostridium* (Figure 4). In the
378 mesophilic FBR, microorganisms of the genus *Clostridium* and *Ruminiclostridium* dominated the

active microbial community at 37 °C (Figure 4). Increasing the FBR temperature to 55 °C resulted in a shift of the active microbial community towards the *Thermoanaerobacterium* genus (> 90% of the relative abundance).

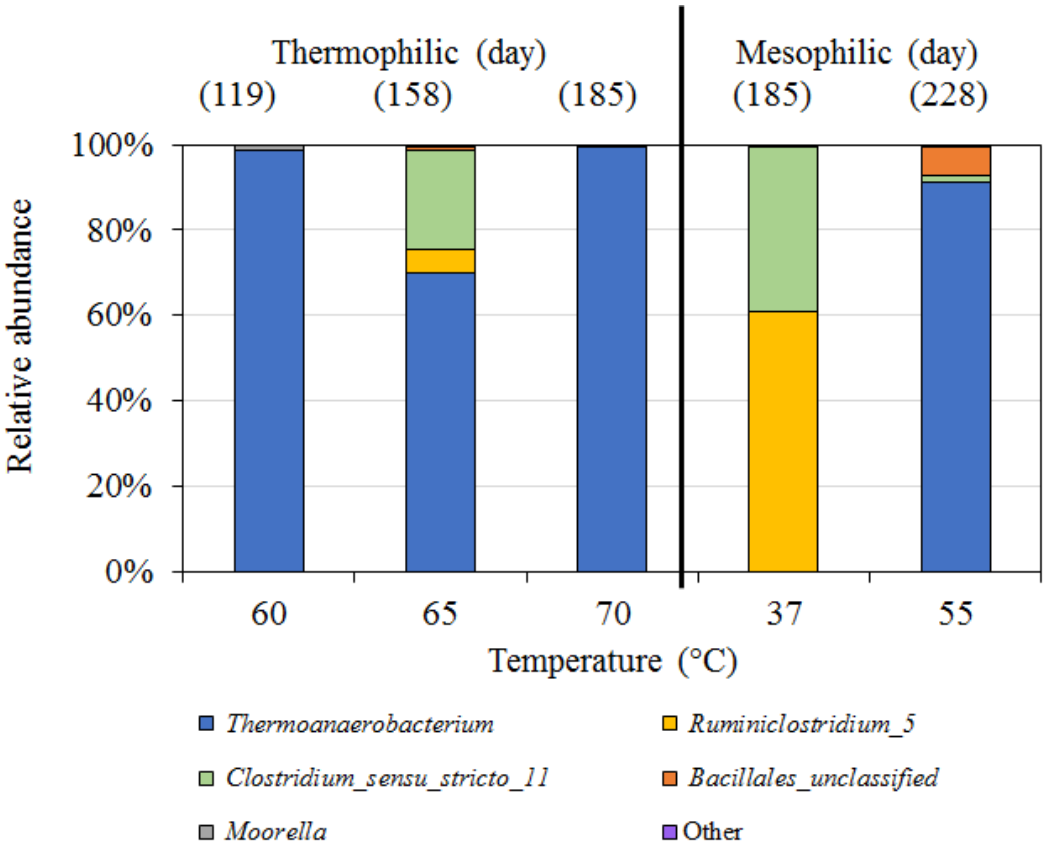

Figure 4. Relative abundance of the active microbial community, classified at genus level, obtained by MiSeq sequencing analysis of the 16S rRNA from biofilm-containing activated carbon samples, reverse transcribed to 16S cDNA. "Other" refers to the sum of genus with a relative abundance < 1%.

4. Discussion

4.1 Thermophilic H_2 production and microbial community dynamics

The significantly higher and more stable H_2 yield obtained when performing dark fermentation of xylose under thermophilic than under mesophilic conditions (Figure 2a versus 2b) was mainly due

393 to the composition of the microbial community (Figure 3; Table 1), particularly the active microbial
394 community (Figure 4). Generally, thermophilic microorganisms yield more H_2 than mesophilic
395 species [5]. A thermophilic community dominated by *Thermoanaerobacterium*, the prevalent active
396 genus in the thermophilic FBR regardless of the temperature applied (Figure 4), has already been
397 reported to yield more H_2 than a mesophilic community dominated by *Clostridium* [49].
398 Furthermore, thermophilic conditions are not favourable for most H_2 consuming microorganisms
399 [27].
400
401 For all the temperatures investigated (55–70 °C), the thermophilic microbial community was
402 dominated by microorganisms closely related to *Thermoanaerobacter thermosaccharolyticum*
403 (Figure 3; Table 1). Accordingly, the genus *Thermoanaerobacterium* was prevailing in the active
404 thermophilic microbial community at 60, 65 and 70 °C (Figure 4). In the thermophilic FBR,
405 although the sample at 55 °C is missing in the active microbial community analysis (Figure 4), the
406 DGGE profile (Figure 3) and the reactor performance (Figure 2a), suggest that
407 *Thermoanaerobacterium* was also the prevalent active genus at 55 °C. In fact, even in the
408 mesophilic FBR, *Thermoanaerobacterium* became dominant upon increasing the temperature from
409 37 to 55 °C (Figure 4). *T. thermosaccharolyticum* has been utilised in batch reactors to produce H_2
410 from xylose at various temperatures, obtaining a maximum yield of about 2.2 mol H_2 mol^{-1} xylose
411 at 60 °C [59,60]. However, in this study, the highest H_2 yield was only about 1.2 mol H_2 mol^{-1}
412 xylose at 55 °C and even 30% lower at 60 °C (Figure 2a), although DGGE profiles appear similar
413 (Figure 3). One explanation is that, in this study, the pH was set to 5.0, whereas the optimum pH for
414 *T. thermosaccharolyticum* is 6.5 [60]. Furthermore, Koskinen et al. [51] showed that in a
415 mesophilic H_2-producing FBR, the attached microbial community is slightly different from the
416 suspended one, which was not analysed in this study. It is thus plausible that the contribution of
417 some H_2 producing or H_2 consuming microorganisms on the net H_2 yield was not considered.

In the thermophilic FBR, sequences belonging to the *Clostridium* genus were detected only at 65 °C, accounting for 22% of the active microbial community (Figure 4). However, at 65 °C, *Clostridium* was not detected by PCR-DGGE. A possible explanation is that the concentration of *Clostridium* was under the detection limit of PCR-DGGE, but these microorganisms were particularly active at 65 °C and thus detected through the RNA-level sequencing analysis [48]. The activity of *Clostridium* is likely linked to the unstable H_2 yield obtained at 65 °C, as some *Clostridium* sp., such as the thermophilic *C. thermoaceticum*, may oxidize sugars through competitive pathways to H_2 or can even carry out homoacetogenesis [61]. The role of *Clostridium* in the xylose degradation at 65 °C could be further detailed by a proteomics analysis. At 65 °C, a bacterium closely related to *Alicyclobacillus* sp. appeared in the DGGE profile (Figure 3). Genera with high similarity (99%) to *Alyciclobacillus* sp. have been found in a thermophilic FBR used for dark fermentation of cheese whey [62], but further studies are required to understand the role of this microorganism in the anaerobic processes.

The drop and subsequent increase in H_2 yield that occurred during the first days of operation at 70 °C, as well as the decreased xylose removal efficiency during these days (Figure 2a and 2c) can be attributed to the acclimation of the microbial community to the higher temperature. Meng et al. [63] performed a proteomic study on *Thermoanaerobacter tengcongensis*, cultured at 55, 75 and 80 °C, and showed the existence of temperature-dependent protein complexes, which may affect the H_2 yield. The stable H_2 yield obtained at 70 °C after the acclimation (Figure 2a) is due to the homogeneity of the active microbial community growing on the carrier material at that temperature: > 99% of the total cDNA sequences matched the genus *Thermoanaerobacterium* (Figure 4).

442 According to the statistical analysis, the highest yield of 1.2 mol H_2 mol^{-1} xylose was obtained at
443 both 55 and 70 °C, whereas the H_2 yield was significantly lower (0.8 mol H_2 mol^{-1} xylose) at 60 and
444 65 °C. Similarly, Yokoyama et al. [30] studied, in batch, dark fermentation of cow waste in the
445 temperature range 37–85 °C, obtaining the highest H_2 production at 60 °C and 75 °C, and a lower
446 H_2 production at 67 °C. However, their cultures were dominated by *Clostridium* sp. and
447 *Caldanaerobacter* sp. at 60 and 75 °C, respectively, in contrast to this study with
448 *Thermoanaerobacter* sp. as the dominant microorganism at both 55 and 70 °C.
449
450 *4.2 Mesophilic H_2 production and microbial community dynamics*
451 The lower H_2 yield obtained under mesophilic conditions (Figure 2b) was attributed to the microbial
452 community. The DGGE profiles obtained on days 119, 158, and 185 were similar to each other and
453 mainly composed of *Clostridium* (Figure 3; Table 1), which was also shown to be the dominant
454 active genus together with the closely related *Ruminiclostridium* genus (Figure 4). Similarly, Si et
455 al. [64] studied the microbial diversity of their mesophilic H_2 producing reactors by MiSeq
456 sequencing, reporting *Clostridiaceae* as the most abundant family. Chatellard et al. [65] showed that
457 *Clostridium*, in particular, dominated mesophilic microbial communities fermenting pentose-based
458 substrates, as was also the case in this study.
459
460 Mesophilic H_2 production was unstable (Figure 2b), likely due to the accumulation of fermentation
461 products, mainly acetate and butyrate, which were produced at a too high rate to be flushed out with
462 the effluent (Figure 2d). At high concentrations, undissociated VFAs penetrate the cell membrane,
463 lowering the internal pH and inhibiting H_2 production [15]. In fact, the H_2 yield (as well as the
464 acetate and butyrate concentration) cyclically increased and decreased in the mesophilic FBR
465 between days 91–185, and the H_2 yield was higher when the concentration of VFAs was lower
466 (Figure 2b and 2d). Wang et al. [66] reported a decrease in H_2 yield at acetate concentrations higher

than 50 mM. In this study, a drop in H_2 yield occurred at acetate concentrations of 40 mM, and the H_2 yield started to increase again when the acetate concentration was about 20-25 mM.

The significantly higher H_2 yield obtained after increasing the temperature of the mesophilic FBR from 37 to 55 °C (Figure 2b) is clearly due to the shift in the active microbial community from the *Clostridium* and *Ruminiclostridium* genus to the *Thermoanaerobacterium* genus (Figure 4). Interestingly, the H_2 yield at 55 °C remained comparable to the one obtained at 37 °C for 13 days, suggesting that the change in the dominant active community did not occur immediately upon the temperature change. The production of ethanol upon exposing the microbial community to 55 °C, and the subsequent shift to acetate, butyrate and H_2 production, was observed also in the first days of operation in the thermophilic FBR (days 1-20, Figure 2c) and in a previous batch study with the same inoculum [18]. This can be attributed to either a change in the microbial community or a gradual shift from ethanol to butyrate fermentation as a response to the temperature shift [18].

4.3 The role of homoacetogenesis on mesophilic and thermophilic H_2 yield

A decrease in H_2 yield to below 0.2 mol H_2 mol^{-1} xylose occurred in the mesophilic FBR on days 9, 16, 74, and 89 (Figure 2b). On the same days, the CO_2 concentration also decreased (File S2 in the supporting material) and a peak of 35–50 mM acetate was detected within 1–2 days from the H_2 decrease (Figure 2d), suggesting the occurrence of homoacetogenesis. H_2 and CO_2 were likely consumed to produce acetate autotrophically. Several *Clostridium* sp., which dominated the active mesophilic microbial community, are known homoacetogens [67]. The causes that trigger microorganisms from heterotrophic to the less energy yielding autotrophic metabolism are controversial. A H_2 partial pressure > 500 Pa can favour homoacetogenesis [10] and H_2 can be simultaneously produced and consumed, but radioactive label tracking techniques would be required to distinguish the two processes [10]. Oh et al. [68] argued that in mixed culture

492 fermentation, the switch to autotrophic metabolism occurs only after substrate depletion. This
493 hypothesis seems less probable in the studied FBR, as xylose was fed continuously. However, it is
494 plausible that H_2 producing microorganisms quickly consume the xylose, inducing the facultative
495 bacteria to shift to autotrophic metabolism.
496
497 Koskinen et al. [51] studied the microbial community dynamics over time in a mesophilic (35 °C)
498 FBR reactor inoculated with digested activated sludge and concluded that the adhesion of H_2
499 consuming microorganisms, including homoacetogens, to the carrier material may cause an
500 unstable H_2 production. Similarly to this study, Dinamarca and Bakke [69] reported a decrease from
501 1.5 to below 0.25 mol H_2 mol^{-1} glucose after 57 days of reactor operation at 35 °C. The authors
502 concluded that homoacetogenesis is directly correlated with the HRT and dependent on biomass
503 density and sludge age [69]. Also Luo et al. [49] argued that, even if the inoculum is pre-treated,
504 methanogenic and homoacetogenic microorganisms could develop again during long-term
505 operation. Methanogens are typically inhibited by a pH below 6, while homoacetogenic bacteria are
506 also inhibited by a pH below 6, but only under thermophilic conditions [49].
507
508 In the thermophilic FBR, excluding day 161 on which a decrease in H_2 yield was attributed to the
509 increased temperature, sudden drops in H_2 yield were not observed (Figure 2a) and the acetate
510 concentration was more stable (Figure 2c). This indicates a minor role of homoacetogenesis at
511 thermophilic conditions. This is in agreement with Luo et al. [49], who reported no
512 homoacetogenesis in thermophilic (55 °C) batch incubations at pH 5.5. Their thermophilic
513 microbial community was dominated by *Thermoanaerobacter* sp., as was the case in this study.
514
515 *4.4 Comparison of H_2 production with previous studies*

516 At 55 °C, despite the HRT of only 6 hours, the H_2 yield per mol xylose added is consistent with a
517 previous batch study with the same inoculum and substrate [18]. At 70 °C, however, H_2 was
518 effectively produced during FBR operation, but not in the batch incubation [18], likely due to the
519 longer time for acclimation of the biomass to the high temperature. The maximum H_2 production
520 rate (HPR) of 282.1 mL H_2 h^{-1} L^{-1} obtained at 70 °C is among the highest reported in continuous
521 studies on thermophilic dark fermentation of sugars by mixed cultures (Table 2). This is likely due
522 to the composition of the active microbial community dominated by an effective H_2 producer such
523 as *Thermoanaerobacterium* (Figure 4). A 12-times higher HPR (3470 mL H_2 h^{-1} L^{-1}) has been
524 obtained with a pure culture of *T. thermosaccharolyticum* immobilized on heat-treated
525 methanogenic granules [70], but the sugar concentration (in terms of chemical oxygen demand) was
526 almost 3 times higher than the concentration used in this study. Furthermore, O-Thong et al. [70]
527 obtained the maximum HPR at an HRT of only 1 hour, whereas in this study the HRT was set to 6
528 hours.
529
530
531
532
533
534
535
536
537
538
539
540
541
542

543 **Table 2.** Highest stable H_2 production rate (HPR) obtained by dark fermentation of simple sugars in various continuous

544 studies conducted at high temperature (T ≥ 55°C) and using different inoculum, reactor type, pH and HRT.

Inoculum	**Pre-treatment**	**Reactor type[a]**	**Substrate (g COD L^{-1})**	**T (°C)**	**pH[b]**	**HRT (h)**	**HPR (mL H_2 h^{-1} L^{-1})**	**Reference**
Biomass from H_2 producing CSTR	-	UASB	Sucrose (11.2)	55	4.5-5.0 (nc)	3	112.5	[33]
Sludge from anaerobic digester	Heat treatment (105°C, 5 min)	UASB	Sucrose (11.2)	55	5.0-5.5 (nc)	1.5	124.2	[24]
Sludge from H_2 producing reactor	Heat treatment (80°C, 60min)	FBR	Sucrose (5.0)	60	5.5 (i)	12	60.5	[34]
Biomass from H_2 producing CSTR	-	TBR	Glucose (7.3)	60	5.5 (c)	2	980.6	[35]
Thermoanaerobacter thermosaccharolyticum immobilised on methanogenic granules	Heat treatment (121°C, 30min)	UASB	Sucrose (22.5)	60	5.0-5.5 (nc)	1	3470	[70]
Biomass from H_2 producing CSTR	-	CSTR	Xylose (1.1)	70	6.7 (nc)	72	2.6	[36]
Biomass from H_2 producing CSTR	-	UASB	Glucose (2.1)	70	7.0 (i)	24	12.7	[37]
Methanogenic biomass from CSTR	Chemical treatment (BES)[c]	UASB	Glucose (4.8)	70	7.2 (i)	27	47.3	[38]
Biomass from H_2 producing CSTR	-	CSTR	Glucose (4.6)	70	5.5 (c)	21.6	91.7	[39]
Activated sludge	Heat treatment (90°C, 15 min)	FBR	Xylose (8.0)	70	5.0 (c)	6	282.1	This study
Caldicellulosiruptor saccharolyticus	-	TBR	Sucrose (11.5)	73	6.5 (c)	3-5	493.1[d]	[71]

545 [a] Continuous stirred tank reactor (CSTR), expanded granular sludge blanket (EGSB), fluidised bed reactor (FBR),
546 sequential batch reactor (SBR), trickling bed reactor (TRB), upflow anaerobic sludge blanket (UASB).
547 [b] The reported pH refers either to the initial pH (i) or the operation pH, which can be either controlled to a stable value
548 (c) or not controlled (nc).
549 [c] Added to the reactor feeding.
550 [d] Per L of filtering bed.
551

552 *4.5 Practical implications*

Organic carbon-rich wastewaters are produced by industries at various temperatures. The energy gain from combustion of the H_2 produced and the energy required to heat the FBR to the desired temperature are two important aspects to take into consideration for a proper economic analysis. For a rough estimation of the effect of operation and feed wastewater temperature on energy gain of a H_2 producing system, a correlation between the wastewater temperature, fermentation temperature and net energy gain is presented in Figure 5.

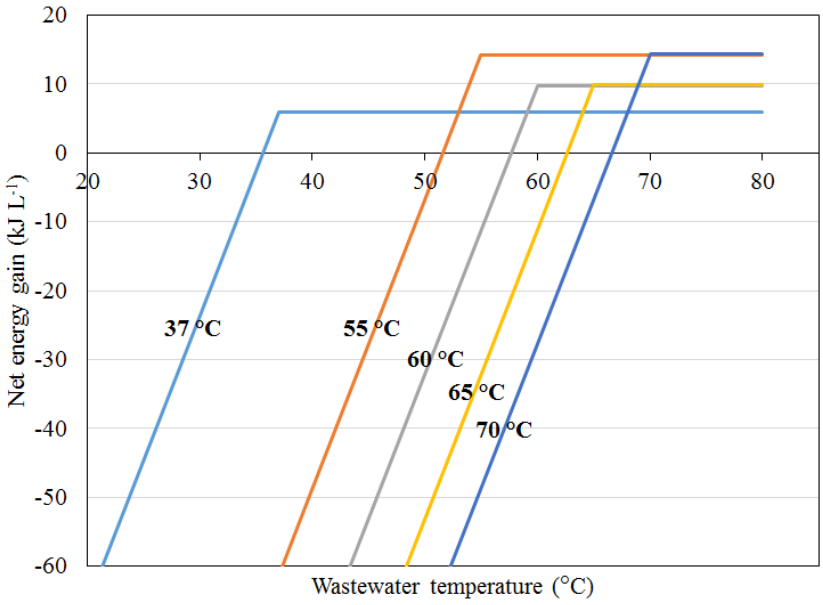

Figure 5. Effect of fermentation temperature on net energy gain from a xylose containing wastewater. X-axis shows the hypothetical temperature at which the wastewater is released. The coloured lines represent the net energy gain obtainable per litre of xylose (50 mM) containing wastewater treated under mesophilic (37 °C) or thermophilic (55, 60, 65, 70 °C) conditions. The net energy gain was calculated according to Perera et al. [41] from the average H_2 yields of the last 4 sampling points collected at the various temperatures investigated in both the mesophilic and thermophilic FBR (8-10 operation days).

570 Despite the comparatively low H_2 yield obtained (Figure 2b), dark fermentation at 37 °C is still the
571 best option to treat wastewaters produced at temperatures up to about 50 °C based on the net energy
572 gain. Thermophilic treatment at 55 °C is to be preferred for wastewaters produced at above 50 °C,
573 and the net energy gain obtained at 70 °C is comparable to the one obtained at 55 °C for
574 wastewaters produced at temperatures exceeding 70 °C (Figure 5). Thermophilic processes could
575 thus be advantageous to treat wastewaters produced at high temperature. However, many other
576 aspects can influence the net energy gain both in a positive (heat recovery from hot wastewater,
577 energy content of the effluent and removal of pathogens) or negative (heat losses, H_2 to energy
578 conversion efficiency and maintenance and operation costs of the FBRs) way.
579
580 The data presented in this study, both on FBR performance and composition of the active microbial
581 community, helps understanding the process and selecting the operation temperature in H_2
582 producing bioreactors depending on the temperature of the waste stream to be treated. However,
583 more research is required to further increase the net energy gain. Post-treatment of the dark
584 fermentation effluent for recovery of value-added products such as VFAs and alcohols or for further
585 energy harvesting (e.g., H_2 production through photo-fermentation or microbial electrolysis cells,
586 methane production through anaerobic digestion or bioelectricity production using microbial fuel
587 cells) is a key factor towards process scale-up [7,72].
588
589 **5. Conclusions**
590 *Thermoanaerobacterium* dominated the thermophilic active microbial community, resulting in a
591 higher and more stable H_2 yield in the thermophilic FBR compared to the mesophilic FBR
592 dominated by *Clostridium*. Treating high temperature, xylose-containing wastewaters by
593 thermophilic dark fermentation can thus lead to a higher energy output compared to the mesophilic
594 counterpart. Temperatures of 55 and 70 °C resulted in the net maximum H_2 yield of 1.2 mol H_2 mol^-

595 [1] xylose, whereas the competition by *Clostridium* caused unstable H_2 production at 65 °C. This
596 study contributes to the understanding of dark fermentation of xylose in FBRs, and the
597 microorganisms actively involved in the mesophilic or thermophilic process, which supports the
598 development of high rate H_2 producing bioreactors.
599
600 **Founding**
601 This work was supported by the Marie Skłodowska-Curie European Joint Doctorate (EJD) in
602 Advanced Biological Waste-To-Energy Technologies (ABWET) funded from Horizon 2020 under
603 grant agreement no. 643071.
604
605 **Conflict of interest**
606 The authors declare no conflict of interest.
607
608 **Acknowledgements**
609 The authors thank Antti Nuottajärvi (TUT, Finland) for helping in the preparation of reactor set-up
610 and Viinikanlahti municipal wastewater treatment plant (Tampere, Finland) for providing the
611 activated sludge.
612
613 **References**
614 [1] Hallenbeck PC, Abo-Hashesh M, Ghosh D. Strategies for improving biological hydrogen
615 production. Bioresour Technol 2012;110:1–9.
616 [2] Nikolaidis P, Poullikkas A. A comparative overview of hydrogen production processes.
617 Renew Sustain Energy Rev 2017;67:597–611.
618 [3] Arimi MM, Knodel J, Kiprop A, Namango SS, Zhang Y, Geißen S-U. Strategies for
619 improvement of biohydrogen production from organic-rich wastewater: A review. Biomass

620 and Bioenergy 2015;75:101–18.
621 [4] Van Groenestijn JW, Hazewinkel JHO, Nienoord M, Bussmann PJT. Energy aspects of
622 biological hydrogen production in high rate bioreactors operated in the thermophilic
623 temperature range. Int J Hydrogen Energy 2002;27:1141–7.
624 [5] Lee D-J, Show K-Y, Su A. Dark fermentation on biohydrogen production: Pure culture.
625 Bioresour Technol 2011;102:8393–402.
626 [6] Vipotnik Z, Jessen JE, Scully SM, Orlygsson J. Effect of culture conditions on hydrogen
627 production by *Thermoanaerobacter* strain AK68. Int J Hydrogen Energy 2016;41:181–9.
628 [7] Ghimire A, Frunzo L, Pirozzi F, Trably E, Escudie R, Lens PNL, et al. A review on dark
629 fermentative biohydrogen production from organic biomass: Process parameters and use of
630 by-products. Appl Energy 2015;144:73–95.
631 [8] Pawar SS, van Niel EWJ. Thermophilic biohydrogen production: how far are we? Appl
632 Microbiol Biotechnol 2013;97:7999–8009.
633 [9] Thauer RK, Jungermann K, Decker K. Energy conservation in chemotrophic anaerobic
634 bacteria. Bacteriol Rev 1977;41:100–80.
635 [10] Saady NMC. Homoacetogenesis during hydrogen production by mixed cultures dark
636 fermentation: Unresolved challenge. Int J Hydrogen Energy 2013;38:13172–91.
637 [11] Angenent LT, Karim K, Al-dahhan MH, Wrenn BA, Domı R. Production of bioenergy and
638 biochemicals from industrial and agricultural wastewater. Trends Biotechnol 2004;22:477–
639 85.
640 [12] Barca C, Soric A, Ranava D, Giudici-Orticoni M-T, Ferrasse J-H. Anaerobic biofilm reactors
641 for dark fermentative hydrogen production from wastewater: a review. Bioresour Technol
642 2015;185:386–98.
643 [13] Li C, Fang HHP. Fermentative Hydrogen Production From Wastewater and Solid Wastes by
644 Mixed Cultures. Crit Rev Environ Sci Technol 2007;37:1–39.

[14] Hüsemann MHW, Papoutsakis ET. Solventogenesis in *Clostridium Acetobutylicum* Fermentations Related to Carboxylic Acid and Proton Concentrations. Biotechnol Bioeng 1988;32:843–52.

[15] Bundhoo MAZ, Mohee R. Inhibition of dark fermentative bio-hydrogen production: A review. Int J Hydrogen Energy 2016;41:6713–33.

[16] Bundhoo MAZ, Mohee R, Hassan MA. Effects of pre-treatment technologies on dark fermentative biohydrogen production: A review. J Environ Manage 2015;157:20–48.

[17] Pradhan N, Dipasquale L, d'Ippolito G, Panico A, Lens PNL, Esposito G, et al. Hydrogen production by the thermophilic bacterium *Thermotoga neapolitana*. Int J Mol Sci 2015;16:12578–600.

[18] Dessì P, Lakaniemi A-M, Lens PNL. Biohydrogen production from xylose by fresh and digested activated sludge at 37, 55 and 70 °C. Water Res 2017;115:120–9.

[19] Ratkowsky DA, Olley J, McMeekin TA, Ball A. relationship between temperature and growth rate of bacterial cultures. J Bacteriol 1982;149:1–5.

[20] Verhaart MRA, Bielen AAM, van der Oost J, Stams AJM, Kengen SWM. Hydrogen production by hyperthermophilic and extremely thermophilic bacteria and archaea: mechanisms for reductant disposal. Environ Technol 2010;31:993–1003.

[21] Kargi F, Eren NS, Ozmihci S. Bio-hydrogen production from cheese whey powder (CWP) solution: comparison of thermophilic and mesophilic dark fermentations. Int J Hydrogen Energy 2012;37:8338–42.

[22] Zheng H-S, Guo W-Q, Yang S-S, Feng X-C, Du J-S, Zhou X-J, et al. Thermophilic hydrogen production from sludge pretreated by thermophilic bacteria: Analysis of the advantages of microbial community and metabolism. Bioresour Technol 2014;172:433–7.

[23] Lin C-Y, Wu C-C, Wu J-H, Chang F-Y. Effect of cultivation temperature on fermentative hydrogen production from xylose by a mixed culture. Biomass and Bioenergy

2008;32:1109–15.

[24] Keskin T, Aksöyek E, Azbar N. Comparative analysis of thermophilic immobilized biohydrogen production using packed materials of ceramic ring and pumice stone. Int J Hydrogen Energy 2011;36:15160–7.

[25] Gokfiliz P, Karapinar I. The effect of support particle type on thermophilic hydrogen production by immobilized batch dark fermentation. Int J Hydrogen Energy 2017;42:2553–61.

[26] Ghimire A, Luongo V, Frunzo L, Pirozzi F, Lens PNL, Esposito G. Continuous biohydrogen production by thermophilic dark fermentation of cheese whey: Use of buffalo manure as buffering agent. Int J Hydrogen Energy 2017;42:4861–9.

[27] Hasyim R, Imai T, Reungsang A, O-Thong S. Extreme-thermophilic biohydrogen production by an anaerobic heat treated digested sewage sludge culture. Int J Hydrogen Energy 2011;36:8727–34.

[28] Mahmod SS, Jahim JM, Abdul PM. Pretreatment conditions of palm oil mill effluent (POME) for thermophilic biohydrogen production by mixed culture. Int J Hydrogen Energy 2017;42:27512–22.

[29] Fangkum A, Reungsang A. Biohydrogen production from mixed xylose/arabinose at thermophilic temperature by anaerobic mixed cultures in elephant dung. Int J Hydrogen Energy 2011;36:13928–38.

[30] Yokoyama H, Waki M, Moriya N, Yasuda T, Tanaka Y, Haga K. Effect of fermentation temperature on hydrogen production from cow waste slurry by using anaerobic microflora within the slurry. Appl Microbiol Biotechnol 2007;74:474–83.

[31] Puhakka JA, Karadag D, Nissilä ME. Comparison of mesophilic and thermophilic anaerobic hydrogen production by hot spring enrichment culture. Int J Hydrogen Energy 2012;37:16453–9.

[32] Mäkinen AE, Nissilä ME, Puhakka JA. Dark fermentative hydrogen production from xylose by a hot spring enrichment culture. Int J Hydrogen Energy 2012;37:12234–40.

[33] Keskin T, Giusti L, Azbar N. Continuous biohydrogen production in immobilized biofilm system versus suspended cell culture. Int J Hydrogen Energy 2012;37:1418–24.

[34] Lutpi NA, Md Jahim J, Mumtaz T, Harun S, Abdul PM. Batch and continuous thermophilic hydrogen fermentation of sucrose using anaerobic sludge from palm oil mill effluent via immobilisation technique. Process Biochem 2016;51:297–307.

[35] Oh Y-K, Kim SH, Kim M-S, Park S. Thermophilic biohydrogen production from glucose with trickling biofilter. Biotechnol Bioeng 2004;88:690–8.

[36] Kongjan P, Min B, Angelidaki I. Biohydrogen production from xylose at extreme thermophilic temperatures (70 °C) by mixed culture fermentation. Water Res 2009;43:1414–24.

[37] Zheng H, Zeng RJ, Angelidaki I. Biohydrogen production from glucose in upflow biofilm reactors with plastic carriers under extreme thermophilic conditions (70°C). Biotechnol Bioeng 2008;100:1034–8.

[38] Kotsopoulos TA, Zeng RJ, Angelidaki I. Biohydrogen production in granular up-flow anaerobic sludge blanket (UASB) reactors with mixed cultures under hyper-thermophilic temperature (70°C). Biotechnol Bioeng 2006;94:296–302.

[39] Zhang F, Chen Y, Dai K, Zeng RJ. The chemostat study of metabolic distribution in extreme-thermophilic (70 °C) mixed culture fermentation. Appl Microbiol Biotechnol 2014;98:10267–73.

[40] Kumar G, Sivagurunathan P, Sen B, Mudhoo A, Davila-Vazquez G, Wang G, et al. Research and development perspectives of lignocellulose-based biohydrogen production. Int Biodeterior Biodegradation 2017;119:225–38.

[41] Perera KRJ, Ketheesan B, Gadhamshetty V, Nirmalakhandan N. Fermentative biohydrogen

720 production: evaluation of net energy gain. Int J Hydrogen Energy 2010;35:12224–33.
721 [42] Suvilampi J, Lepistö R, Rintala J. Biological treatment of pulp and paper mill process and
722 wastewaters under thermophilic conditions – A review. Pap Timber 2001;83:320–5.
723 [43] Cavalcante de Amorim EL, Barros AR, Rissato Zamariolli Damianovic MH, Silva EL.
724 Anaerobic fluidized bed reactor with expanded clay as support for hydrogen production
725 through dark fermentation of glucose. Int J Hydrogen Energy 2009;34:783–90.
726 [44] Karadag D, Puhakka JA. Effect of changing temperature on anaerobic hydrogen production
727 and microbial community composition in an open-mixed culture bioreactor. Int J Hydrogen
728 Energy 2010;35:10954–9.
729 [45] Etchebehere C, Castelló E, Wenzel J, del Pilar Anzola-Rojas M, Borzacconi L, Buitrón G, et
730 al. Microbial communities from 20 different hydrogen-producing reactors studied by 454
731 pyrosequencing. Appl Microbiol Biotechnol 2016;100:3371–84.
732 [46] Nitipan S, Mamimin C, Intrasungkha N, Birkeland NK, O-Thong S. Microbial community
733 analysis of thermophilic mixed culture sludge for biohydrogen production from palm oil mill
734 effluent. Int J Hydrogen Energy 2014;39:19285–93.
735 [47] Zhang F, Yang J-H, Dai K, Ding Z-W, Wang L-G, Li Q-R, et al. Microbial dynamics of the
736 extreme-thermophilic (70 °C) mixed culture for hydrogen production in a chemostat. Int J
737 Hydrogen Energy 2016;41:11072–80.
738 [48] De Vrieze J, Regueiro L, Props R, Vilchez-Vargas R, Jáuregui R, Pieper DH, et al. Presence
739 does not imply activity: DNA and RNA patterns differ in response to salt perturbation in
740 anaerobic digestion. Biotechnol Biofuels 2016;9:244.
741 [49] Luo G, Karakashev D, Xie L, Zhou Q, Angelidaki I. Long-term effect of inoculum
742 pretreatment on fermentative hydrogen production by repeated batch cultivations:
743 homoacetogenesis and methanogenesis as competitors to hydrogen production. Biotechnol
744 Bioeng 2011;108:1816–27.

745 [50] Kinnunen V, Ylä-Outinen a., Rintala J. Mesophilic anaerobic digestion of pulp and paper
746 industry biosludge–long-term reactor performance and effects of thermal pretreatment. Water
747 Res 2015;87:105–11.
748 [51] Koskinen PEP, Kaksonen AH, Puhakka JA. The relationship between instability of H_2
749 production and compositions of bacterial communities within a dark fermentation fluidized-
750 bed bioreactor. Biotechnol Bioeng 2006;97:742–58.
751 [52] Hall T. BioEdit: a user-friendly biological sequence alignment editor and analysis program
752 for Windows 95/98/NT. Nucleic Acids Symp Ser 1999;41:95–8.
753 [53] Altschul SF, Gish W, Miller W, Myers EW, Lipman DJ. Basic local alignment search tool. J
754 Mol Biol 1990;215:403–10. doi:10.1016/S0022-2836(05)80360-2.
755 [54] Griffiths RI, Whiteley AS, O'Donnell AG, Bailey MJ. Rapid method for coextraction of
756 DNA and RNA from natural environments for analysis of ribosomal DNA- and rRNA-based
757 microbial community composition. Appl Environ Microbiol 2000;66:5488–91.
758 [55] Caporaso JG, Lauber CL, Walters WA, Berg-Lyons D, Lozupone CA, Turnbaugh PJ, et al.
759 Global patterns of 16S rRNA diversity at a depth of millions of sequences per sample. Proc
760 Natl Acad Sci U S A 2011;108:4516–22.
761 [56] Schloss PD, Westcott SL, Ryabin T, Hall JR, Hartmann M, Hollister EB, et al. Introducing
762 mothur: open-source, platform-independent, community-supported software for describing
763 and comparing microbial communities. Appl Environ Microbiol 2009;75:7537–41.
764 [57] Kozich JJ, Westcott SL, Baxter NT, Highlander SK, Schloss PD. Development of a dual-
765 index sequencing strategy and curation pipeline for analyzing amplicon sequence data on the
766 miseq illumina sequencing platform. Appl Environ Microbiol 2013;79:5112–20.
767 [58] Box GEP, Holohan R, Scott E. Statistics for experimenters: an introduction to design, data
768 analysis, and model building. John Wiley and sons; 1978.
769 [59] Khamtib S, Reungsang A. Biohydrogen production from xylose by *Thermoanaerobacterium*

770 *thermosaccharolyticum* KKU19 isolated from hot spring sediment. Int J Hydrogen Energy
771 2012;37:12219–28.
772 [60] Ren N, Cao G, Wang A, Lee D, Guo W, Zhu Y. Dark fermentation of xylose and glucose
773 mix using isolated *Thermoanaerobacterium thermosaccharolyticum* W16. Int J Hydrogen
774 Energy 2008;33:6124–32.
775 [61] Koesnandar, Nishio N, Nagai S. Effects of Trace Metal Ions on the Growth,
776 Homoacetogenesis and Corrinoid Production by *Clostridium thermoaceticum*. J Ferment
777 Bioeng 1991;71:181–5.
778 [62] Ottaviano LM, Ramos LR, Botta LS, Amâncio Varesche MB, Silva EL. Continuous
779 thermophilic hydrogen production from cheese whey powder solution in an anaerobic
780 fluidized bed reactor: Effect of hydraulic retention time and initial substrate concentration.
781 Int J Hydrogen Energy 2017;42:4848–60.
782 [63] Meng B, Qian Z, Wei F, Wang W, Zhou C, Wang Z, et al. Proteomic analysis on the
783 temperature-dependent complexes in *Thermoanaerobacter tengcongensis*. Proteomics
784 2009;9:3189–200.
785 [64] Si B, Liu Z, Zhang Y, Li J, Xing X-H, Li B, et al. Effect of reaction mode on biohydrogen
786 production and its microbial diversity. Int J Hydrogen Energy 2015;40:3191–200.
787 [65] Chatellard L, Trably E, Carrère H. The type of carbohydrates specifically selects microbial
788 community structures and fermentation patterns. Bioresour Technol 2016;221:541–9.
789 [66] Wang B, Wan W, Wang J. Inhibitory effect of ethanol, acetic acid, propionic acid and butyric
790 acid on fermentative hydrogen production. Int J Hydrogen Energy 2008;33:7013–9.
791 [67] Ryan P, Forbes C, Colleran E. Investigation of the diversity of homoacetogenic bacteria in
792 mesophilic and thermophilic anaerobic sludges using the formyltetrahydrofolate synthetase
793 gene. Water Sci Technol 2008;57:675–80.
794 [68] Oh S-E, Van Ginkel S, Logan BE. The Relative Effectiveness of pH Control and Heat

795 Treatment for Enhancing Biohydrogen Gas Production. Environ Sci Technol 2003;37:5186–
796 90.
797 [69] Dinamarca C, Bakke R. Apparent hydrogen consumption in acid reactors: observations and
798 implications. Water Sci Technol 2009;59:1441–7.
799 [70] O-Thong S, Prasertsan P, Karakashev D, Angelidaki I. High-rate continuous hydrogen
800 production by *Thermoanaerobacterium thermosaccharolyticum* PSU-2 immobilized on heat-
801 pretreated methanogenic granules. Int J Hydrogen Energy 2008;33:6498–508.
802 [71] Van Groenestijn JW, Geelhoed JS, Goorissen HP, Meesters KPM, Stams AJM, Claassen
803 PAM. Performance and Population Analysis of a Non-Sterile Trickle Bed Reactor Inoculated
804 With *Caldicellulosiruptor saccharolyticus*, a Thermophilic Hydrogen Producer. Biotechnol
805 Bioeng 2009;102:1361–7.
806 [72] Sharma Y, Li B. Optimizing energy harvest in wastewater treatment by combining anaerobic
807 hydrogen producing biofermentor (HPB) and microbial fuel cell (MFC). Int J Hydrogen
808 Energy 2010;35:3789–97.
809

File S1. Statistical analysis (ANOVA and Tukey test) conducted at p = 0.05 to asses significant differences in H_2 yield at the various temperatures investigated in the mesophilic (37 – 55 °C) and thermophilic (55 – 70 °C) FBR. The analysis was conducted on the last 4 sampling points (10-12 days) collected at each temperature.

Descriptives

FBR	T (°C)	N	Mean H_2 yield	Std. Deviation	Std. Error	95% Confidence Interval for Mean		Minimum	Maximum
						Lower Bound	Upper Bound		
Mesophilic	37	4	0.4586	0.02465	0.01233	0.4194	0.4978	0.43	0.49
	55	4	1.0040	0.02961	0.01481	0.9568	1.0511	0.97	1.03
Thermophilic	55	4	1.1855	0.04847	0.02424	1.1083	1.2626	1.12	1.23
	60	4	0.8221	0.02957	0.01479	0.7751	0.8692	0.79	0.85
	65	4	0.8197	0.11724	0.05862	0.6332	1.0063	0.69	0.97
	70	4	0.2139	0.03945	0.01973	1.1511	1.2767	1.17	1.26
	Total	24	0.9173	0.26748	0.05460	0.8043	1.0302	0.43	1.26

ANOVA

	Sum of Squares	df	Mean Square	F	Sig.
Between Groups	1.586	5	0.317	95.077	0.000
Within Groups	0.060	18	0.003		
Total	1.646	23			

Multiple comparisons

Multiple Comparisons

Dependent Variable: Yield

Tukey HSD

(I) Temperature	(J) Temperature	Mean Difference (I-J)	Std. Error	Sig.	95% Confidence Interval	
					Lower Bound	Upper Bound
37 (M) **	55 (M)	-0.54537*	0.04084	0.000	-0.6751	-0.4156
	55 (T)	-0.72689*	0.04084	0.000	-0.8567	-0.5971
	60 (T)	-0.36356*	0.04084	0.000	-0.4933	-0.2338
	65 (T)	-0.36115*	0.04084	0.000	-0.4909	-0.2314
	70 (T)	-0.75530*	0.04084	0.000	-0.8851	-0.6255
55 (M)	37 (M)	0.54537*	0.04084	0.000	0.4156	0.6751
	55 (T)	-0.18152*	0.04084	0.004	-0.3113	-0.0517
	60 (T)	0.18181*	0.04084	0.004	0.0520	0.3116
	65 (T)	0.18422*	0.04084	0.003	0.0544	0.3140
	70 (T)	-0.20993*	0.04084	0.001	-0.3397	-0.0801
55 (T)	37 (M)	0.72689*	0.04084	0.000	0.5971	0.8567
	55 (M)	0.18152*	0.04084	0.004	0.0517	0.3113
	60 (T)	0.36333*	0.04084	0.000	0.2335	0.4931
	65 (T)	0.36574*	0.04084	0.000	0.2360	0.4955
	70 (T)	-0.02841	0.04084	0.980	-0.1582	0.1014
60.00 (T)	37 (M)	0.36356*	0.04084	0.000	0.2338	0.4933
	55 (M)	-0.18181*	0.04084	0.004	-0.3116	-0.0520
	55 (T)	-0.36333*	0.04084	0.000	-0.4931	-0.2335
	65 (T)	0.00242	0.04084	1.000	-0.1274	0.1322
	70 (T)	-0.39173*	0.04084	0.000	-0.5215	-0.2620
65.00 (T)	37 (M)	0.36115*	0.04084	0.000	0.2314	0.4909
	55 (M)	-0.18422*	0.04084	0.003	-0.3140	-0.0544
	55 (T)	-0.36574*	0.04084	0.000	-0.4955	-0.2360
	60 (T)	-0.00242	0.04084	1.000	-0.1322	0.1274
	70 (T)	-0.39415*	0.04084	0.000	-0.5239	-0.2644
70.00 (T)	37 (M)	0.75530*	0.04084	0.000	0.6255	0.8851
	55 (M)	0.20993*	0.04084	0.001	0.0801	0.3397
	55 (T)	0.02841	0.04084	0.980	-0.1014	0.1582
	60 (T)	0.39173*	0.04084	0.000	0.2620	0.5215
	65 (T)	0.39415*	0.04084	0.000	0.2644	0.5239

*. The mean difference is significant at the 0.05 level.

**. M = mesophilic FBR. T = thermophilic FBR.

Homogeneous subset

Tukey HSD*

Temperature	N	Subset for alpha = 0.05			
		1	2	3	4
37 (M) **	4	0.4586			
65 (T)	4		0.8197		
60 (T)	4		0.8221		
55 (M)	4			1.0040	
55 (T)	4				1.1855
70 (T)	4				1.2139
Sig.		1.000	1.000	1.000	0.980

Means H_2 yield for groups in homogeneous subsets are displayed.

*. Uses Harmonic Mean Sample Size = 4.000.

**. M = mesophilic FBR. T = thermophilic FBR.

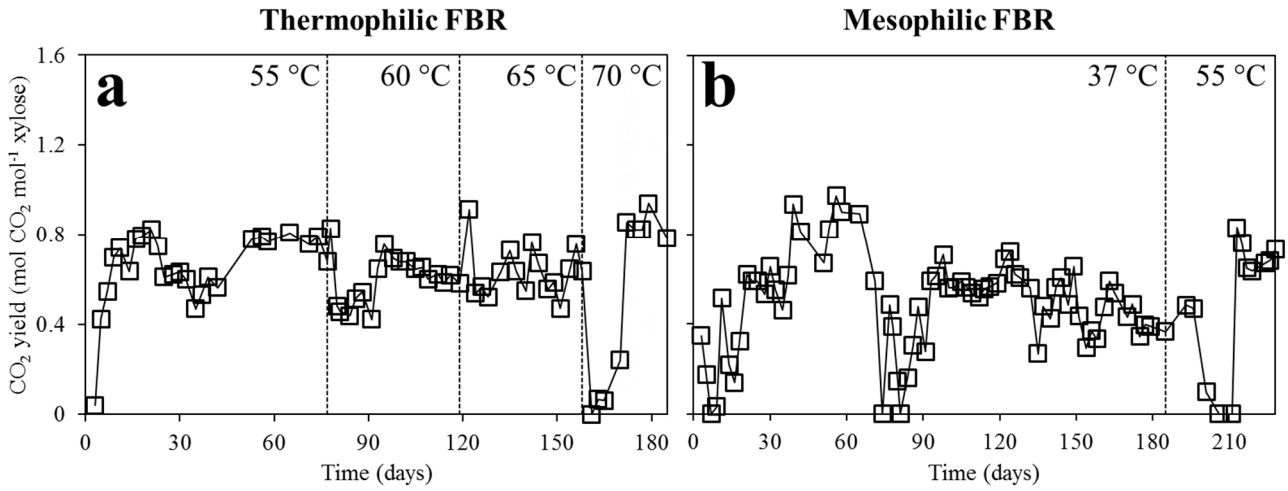

File S2. CO_2 yield (mol CO_2 mol^{-1} xylose added) in the thermophilic (a) and mesophilic (b) FBR. The vertical dotted lines indicate a change of temperature.